A Fokker-Planck description of dense flows

Mohsen Sadr

Supervisors: Dr. Hossein Gorji
Prof. Manuel Torrilhon

Computational Engineering Science, Mathematics Division
RWTH Aachen University

February 26, 2018

Outline

1. Introduction
   - Motivation
2. Dense Gases
   - Enskog Equation
   - Fokker-Planck model
   - Validation studies
3. Conclusion

Outline

1. Introduction
   - Motivation
2. Dense Gases
   - Enskog Equation
   - Fokker-Planck model
   - Validation studies
3. Conclusion

Why this topic?

- We want
  an efficient kinetic model that can describe non-equilibrium dilute, dense gases and if possible, phase transition to liquids.

Why this topic?

- We want
  an efficient kinetic model that can describe non-equilibrium dilute, dense gases and if possible, phase transition to liquids.
- **DSMC** based methods (ESMC, ...) become **too expensive** at high densities.
- We need an accurate mathematical model whose **computational cost** has **no correlation with density**.
- Applications: unconventional gas reservoirs, high pressure shock tubes, Sonoluminescence, and interface of liquid-vapor at supercritical pressures.

Collision in dilute .*vs.* dense gases

Dilute

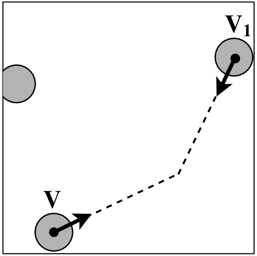

Point particle:
Boltzmann collision operator

Collision in dilute *.vs.* dense gases

Dilute

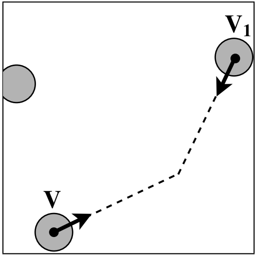

Point particle:
Boltzmann collision operator

Dense

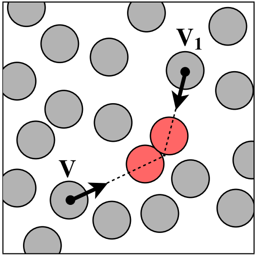

Particles with Sutherland potential:
Enskog collision operator
$+$ **attraction.**

Outline

Enskog equation[1]

Enskog modified Boltzmann equation in order to include dense effects

$$\frac{\partial \mathcal{F}}{\partial t} + \frac{\partial (\mathcal{F} V_i)}{\partial x_i} = S^{\text{Ensk}} , \tag{2.1}$$

where

$$S^{\text{Ensk}} = \int_{\mathbb{R}^3} \int_0^{2\pi} \int_0^{+\infty} \Big[Y(\mathbf{x} + \frac{1}{2}\sigma \hat{\mathbf{k}}) \mathcal{F}(\mathbf{V}^*, \mathbf{x}) \mathcal{F}(\mathbf{V}_1^*, \mathbf{x} + \sigma \hat{\mathbf{k}}) - Y(\mathbf{x} - \frac{1}{2}\sigma \hat{\mathbf{k}}) \mathcal{F}(\mathbf{V}, \mathbf{x}) \mathcal{F}(\mathbf{V}_1, \mathbf{x} - \sigma \hat{\mathbf{k}}) \Big] g \hat{b} d\hat{b} d\hat{\epsilon} d^3 \mathbf{V}_1 . \tag{2.2}$$

- $\hat{b}$, $\hat{\epsilon}$ and $\hat{\mathbf{k}}$ specify collision cross section.
- σ: effective diameter of particles.
- Y: pair correlation function.
- $*$: post-collision state.

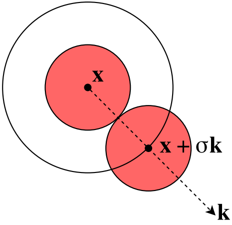

[1] see Chapman, S., & Cowling, T. (1953) and Hirschfelder, J. *et al.* (1963).

Current Monte-Carlo methods

Modifying DSMC (ESMC[2]and Frezzotti's algorithm[3]) such that:

- Collision rate is increased by the factor Y, i.e.

$$\omega_{ij}/\Delta t = 4\pi\sigma^2(\mathbf{k}.\mathbf{g}_{ij})Y(\mathbf{x}+\sigma/2\hat{\mathbf{k}})n_J \tag{2.3}$$

- Colliding pair is selected from cells that enclose $\mathbf{x}$ and $\mathbf{x}+\sigma\hat{\mathbf{k}}$.

[2] see Montanero, J. M., & Santos, A., Physical Review E 54, no. 1 (1996): 438.

[3] see Frezzotti, A. Physics of Fluids 9, no. 5 (1997): 1329-1335.

Current Monte-Carlo methods

Modifying DSMC (ESMC[2]and Frezzotti's algorithm[3]) such that:

- Collision rate is increased by the factor Y, i.e.

$$\omega_{ij}/\Delta t = 4\pi\sigma^2(\mathbf{k}.\mathbf{g}_{ij})Y(\mathbf{x}+\sigma/2\hat{\mathbf{k}})n_J \tag{2.3}$$

- Colliding pair is selected from cells that enclose $\mathbf{x}$ and $\mathbf{x}+\sigma\hat{\mathbf{k}}$.

Problem

Computational complexity of DSMC-based methods increases with density since collision rate of HS is $\omega_{ij}/\Delta t = 4\pi\sigma^2(\mathbf{k}.\mathbf{g}_{ij})Y(\mathbf{x}+\sigma/2\hat{\mathbf{k}})n_J$.

[2] see Montanero, J. M., & Santos, A., Physical Review E 54, no. 1 (1996): 438.

[3] see Frezzotti, A. Physics of Fluids 9, no. 5 (1997): 1329-1335.

Outline

1 Introduction
- Motivation

2 Dense Gases
- Enskog Equation
- Fokker-Planck model
- Validation studies

3 Conclusion

Fokker-Planck model

Consider an Itô process

$$d\mathbf{p} = \widetilde{\mathbf{A}}dt + \boldsymbol{\lambda} d\mathbf{W}, \tag{2.4}$$

where **W** is a Wiener process. Itô calculus provides us the equivalent Fokker-Planck equation[4]

$$\frac{\partial \mathcal{F}}{\partial t} + \frac{\partial(\mathcal{F} V_i)}{\partial x_i} = -\frac{\partial(\mathcal{F} A_i)}{\partial V_i} + \frac{1}{2}\frac{\partial^2}{\partial V_i \partial V_j}(D_{ik} D_{kj} \mathcal{F}). \tag{2.5}$$

Drift and diffusion

A and **D** are called drift and diffusion coefficients, respectively. They are set to give an approximation of a generic collision operator.

[4] see Gardiner, C. W. (1996).

Homogeneous relaxation rates of Enskog equation

- Let us write Enskog operator using the decomposition

$$S^{\text{Ensk}} = Y(\mathbf{x})S^{\text{Boltz}} + S_\phi \tag{2.6}$$

where S_ϕ includes all spatial dependency of $\mathcal{F}$ and Y in $\mathbf{x}$.

- Relaxation rates of shear stress and heat fluxes then become

$$\left.\frac{\partial \pi_{ij}}{\partial t}\right|_{\text{coll}} = -Y\frac{p}{\mu^{\text{kin}}}\pi_{ij} \tag{2.7}$$

$$\text{and} \quad \left.\frac{\partial q_i}{\partial t}\right|_{\text{coll}} = -Y\frac{2}{3}\frac{p}{\mu^{\text{kin}}}q_i\ . \tag{2.8}$$

- Drift **A** and diffusion **D** can be modelled by a cubic FP model proposed by Gorji *et al.* [5] with modifications for dense gases.

[5] Gorji, M. H. and Torrilhon, M. and Jenny, P., Journal of fluid mechanics 680 (2011): 574-601.

Conservation equations of Enskog equation

- Taking velocity moment $\psi \in \{1, V_j, V_j V_j/2\}$ of expanded Enskog equation leads to

$$\int_{\mathbb{R}^3} \psi\Big(\frac{\partial \mathcal{F}}{\partial t} + V_i \frac{\partial \mathcal{F}}{\partial x_i}\Big) d^3\mathbf{V} \quad = -\frac{\partial \Psi_i^{\phi}}{\partial x_i}. \tag{2.9}$$

where $\mathbf{\Psi}^{\phi}$ is called collsional transfer and is defined by

$$\Psi_i^{\phi} = \underbrace{\frac{Y\sigma}{2}\int\int\int\int(\psi^* - \psi)\mathcal{F}\mathcal{F}_1 k_i g \hat{b} d\hat{b} d\hat{\epsilon} d^3\mathbf{V}_1 d^3\mathbf{V}}_{I_1}$$
$$+ \underbrace{\frac{Y\sigma^2}{4}\int\int\int\int(\psi^* - \psi)\mathcal{F}\mathcal{F}_1 \frac{\partial}{\partial x_j} ln\Big(\frac{\mathcal{F}}{\mathcal{F}_1}\Big) k_i k_j g \hat{b} d\hat{b} d\hat{\epsilon} d^3\mathbf{V}_1 d^3\mathbf{V}}_{I_2}$$
$$+ \ldots \tag{2.10}$$

- Unlike Boltzmann, moments of Enskog operator for momentum and energy do not vanish! $\rightarrow$ **collisional transfer**

- Assuming Maxwellian $\mathcal{F}$ in $I_2(\psi)$ and ignoring higher order terms

$$p^{\text{tot}} = (1 + \underbrace{nbY)nkT}_{=I_1} - \underbrace{w\frac{\partial U_k}{\partial x_k}}_{\approx I_2}, \quad (2.11)$$

$$\pi_{ij}^{\text{tot}} = (1 + \underbrace{2nbY/5)\pi_{ij}}_{=I_1} - \underbrace{(5w/6)\frac{\partial U_{\langle i}}{\partial x_{j\rangle}}}_{\approx I_2} \quad (2.12)$$

and

$$q_i^{\text{tot}} = (1 + \underbrace{3nbY/5)q_i}_{=I_1} - \underbrace{c_v w\frac{\partial T}{\partial x_i}}_{\approx I_2} \quad (2.13)$$

with $w = (nb)^2 Y\sqrt{mkT}/(\pi^{3/2}\sigma^2)$ being bulk viscosity.

- We use these expressions to correct total pressure tensor and total heat fluxes in FP of dense gases.

FP with collisional transfer

- Collisional transfer promotes idea of extra streaming

$$\frac{\partial \mathcal{F}}{\partial t} + \frac{\partial(\mathcal{F}V_i)}{\partial x_i} = -\frac{\partial(\mathcal{F}A_i)}{\partial V_i} + \frac{1}{2}\frac{\partial^2(D^2\mathcal{F})}{\partial V_j \partial V_j} - \frac{\partial(\mathcal{F}\hat{A}_i)}{\partial x_i} . \quad (2.14)$$

- What is $\hat{\mathbf{A}}$?
  Answer: $\hat{\mathbf{A}}$ is a spatial drift which should be set such that moments of FP matches moments of Enskog, i.e. provides correction to total pressure tensor and heat fluxes.
- In this study, we proposed a cubic model for $\hat{\mathbf{A}}$, i.e.

$$\hat{A}_i = \hat{c}_{ij} v'_j + \hat{\gamma}_i \left(v'_j v'_j - \frac{3kT}{m} \right) + \hat{\Lambda}\left(v'_i v'_j v'_j - \frac{2q_i}{\rho} \right) \quad (2.15)$$

where $\hat{\Lambda} = -\epsilon nbY/(kT/m)$ is set to avoid instabilities of SDEs.

Cubic FP: conservation equations

- Mass conservation:

$$\frac{\partial \rho}{\partial t} + \frac{\partial (\rho U_i)}{\partial x_i} = 0 \ . \tag{2.16}$$

- Momentum conservation:

$$\begin{aligned} \frac{\partial}{\partial t}(\rho U_i) + \frac{\partial}{\partial x_j}(\rho U_i U_j) + \frac{\partial}{\partial x_j}(\pi_{ij} + p\delta_{ij}) & \\ + \frac{\partial}{\partial x_j} \int_{\mathbb{R}^3} \hat{A}_j V_i \mathcal{F} d^3\mathbf{V} &= 0 \ . \end{aligned} \tag{2.17}$$

- Energy conservation:

$$\begin{aligned} \frac{\partial E}{\partial t} &+ \frac{\partial}{\partial x_i}\left(EU_i + q_i + p\delta_{ik}U_k + \pi_{ik}U_k\right) \\ &+ \frac{1}{2}\frac{\partial}{\partial x_i} \int_{\mathbb{R}^3} \hat{A}_i V_k V_k \mathcal{F} d^3\mathbf{V} = 0. \end{aligned} \tag{2.18}$$

Outline

1. Introduction
   - Motivation
2. Dense Gases
   - Enskog Equation
   - Fokker-Planck model
   - Validation studies
3. Conclusion

Equilibrium Pressure

- Iso-thermal walls with $T_w = 273\ K$.
- Equilibrium pressure can be calculated based on its fundamental definition.

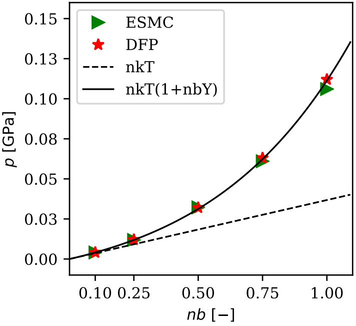

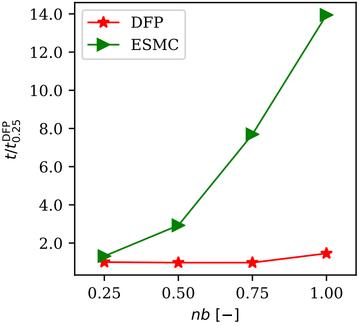

Lid-driven cavity

- Temperature contours and heat fluxes of the lid-driven cavity flow at $\mathrm{Kn} = 0.1$, $nb = 0.1$ and $U_w = 300$ m/s.

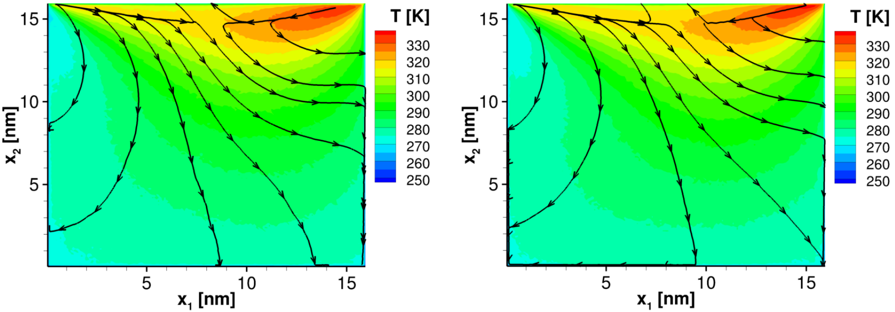

(a) FP (b) ESMC

Conclusion

- We proposed a Fokker-Planck model suitable for dense gases.
- Dense gas effects were captured by introducing a drift in physical space.
- Several examples showed the accuracy of model in capturing total pressure, shear stress and heat fluxes.
- Future studies:
  - Obtaining higher order approximation of collisional transfer.
  - Including attractive part of molecular potential.

Thanks for your attention.

For Further Reading I

- R. Sander, Z. Pan, and L. D. Connell, "Laboratory measurement of low permeability unconventional gas reservoir rocks: A review of experimental methods," *Journal of Natural Gas Science and Engineering*, vol. 37, pp. 248–279, 2017.
- E. L. Petersen and R. K. Hanson, "Nonideal effects behind reflected shock waves in a high-pressure shock tube," *Shock Waves*, vol. 10, no. 6, pp. 405–420, 2001.
- M. P. Brenner, S. Hilgenfeldt, and D. Lohse, "Single-bubble sonoluminescence," *Reviews of Modern Physics*, vol. 74, no. 2, p. 425, 2002.
- R. N. Dahms, J. Manin, L. M. Pickett, and J. C. Oefelein, "Understanding high-pressure gas-liquid interface phenomena in diesel engines," *Proceedings of the Combustion Institute*, vol. 34, no. 1, pp. 1667–1675, 2013.

For Further Reading II

- R. N. Dahms and J. C. Oefelein, "Liquid jet breakup regimes at supercritical pressures," *Combustion and Flame*, vol. 162, no. 10, pp. 3648–3657, 2015.
- R. N. Dahms and J. C. Oefelein, "Non-equilibrium gas–liquid interface dynamics in high-pressure liquid injection systems," *Proceedings of the Combustion Institute*, vol. 35, no. 2, pp. 1587–1594, 2015.
- S. Chapman and T. G. Cowling, *The mathematical theory of non-uniform gases: an account of the kinetic theory of viscosity, thermal conduction and diffusion in gases*. Cambridge university press, 1970.
- J. Hirschfelder, R. B. Bird, and C. F. Curtiss, *Molecular theory of gases and liquids*. Wiley, 1964.

For Further Reading III

- J. M. Montanero and A. Santos, “Monte Carlo simulation method for the Enskog equation,” *Physical Review E*, vol. 54, no. 1, p. 438, 1996.
- A. Frezzotti, “A particle scheme for the numerical solution of the Enskog equation,” *Physics of Fluids*, vol. 9, no. 5, pp. 1329–1335, 1997.
- C. W. Gardiner, *Handbook of stochastic methods: For Physics, Chemistry and the Natural Sciences*, vol. 13. 1996.
- M. H. Gorji, M. Torrilhon, and P. Jenny, “Fokker–Planck model for computational studies of monatomic rarefied gas flows,” *Journal of Fluid Mechanics*, vol. 680, pp. 574–601, 2011.
- F. H. Ree and W. G. Hoover, “Fifth and sixth virial coefficients for hard spheres and hard disks,” *The Journal of Chemical Physics*, vol. 40, no. 4, pp. 939–950, 1964.

For Further Reading IV

- N. F. Carnahan and K. E. Starling, "Equation of state for nonattracting rigid spheres," *The Journal of Chemical Physics*, vol. 51, no. 2, pp. 635–636, 1969.
- W. Wagner, "A convergence proof for Bird's direct simulation Monte Carlo method for the Boltzmann equation," *Journal of Statistical Physics*, vol. 66, no. 3, pp. 1011–1044, 1992.
- G. A. Bird, "Approach to translational equilibrium in a rigid sphere gas," *Physics of Fluids*, vol. 6, no. 10, pp. 1518–1519, 1963.
- F. J. Alexander, A. L. Garcia, and B. J. Alder, "A consistent Boltzmann algorithm," *Physical Review Letters*, vol. 74, no. 26, p. 5212, 1995.

For Further Reading V

P. Jenny, M. Torrilhon, and S. Heinz, "A solution algorithm for the fluid dynamic equations based on a stochastic model for molecular motion," *Journal of Computational Physics*, vol. 229, no. 4, pp. 1077–1098, 2010.

C. Truesdell and R. G. Muncaster, *Fundamentals of Maxwel's Kinetic Theory of a Simple Monatomic Gas: Treated as a Branch of Rational Mechanics*, vol. 83.
Academic Press, 1980.

H. Risken, "The Fokker-Planck equation: Methods of solution and applications," *Springer*, 1989.

M. H. Gorji and P. Jenny, "An efficient particle Fokker–Planck algorithm for rarefied gas flows," *Journal of Computational Physics*, vol. 262, pp. 325–343, 2014.

For Further Reading VI

G. A. Bird, *Molecular Gas Dynamics and the Direct Simulation of Gas Flows.*
Molecular Gas Dynamics and the Direct Simulation of Gas Flows, Clarendon Press, 1994.

M. H. Gorji and P. Jenny, "Fokker–Planck–DSMC algorithm for simulations of rarefied gas flows," *Journal of Computational Physics*, vol. 287, pp. 110–129, 2015.

Outline

Why this topic?

- We want **an efficient model that can describe non-equilibrium dilute, dense gases and if possible, liquid**.
- **DSMC** based methods, such as ESMC and CBA, are **too expensive**.
- Since collisions are not explicitly calculated in **FP model**, it is shown to be **more efficient** than DSMC based methods as Knudsen number decreases which encourages us to extend it for dense gases as well.
- We need a accurate mathematical model that its **computational cost** has **no correlation with density**.
- Applications: unconventional gas reservoirs[1], high pressure shock tubes[2], Sonoluminescence[3] and interface of liquid-vapor at supercritical pressures[4, 5, 6].

Outline

Kinetic Theory

- Let us consider the sample space of $\mathbf{V}$ and $\mathbf{x}$.
- Macroscopic properties can be determined by probability density function $f(\mathbf{V};\mathbf{x},t)$, i.e. probability density of finding a particle close to the velocity $\mathbf{V}$ and conditional on $\mathbf{x}-t$.
- Here, velocity distribution function (VDF) $\mathcal{F}(\mathbf{V},\mathbf{x},t)$ is employed where

$$\mathcal{F}(\mathbf{V},\mathbf{x},t) \quad = \quad \rho(\mathbf{x},t)f(\mathbf{V};\mathbf{x},t), \tag{5.1}$$

Kinetic Theory

- Kinetic Theory provides macroscopic properties as functions of VDF

$$\rho(\mathbf{x}, t) = \int_{R^3} \mathcal{F} d^3\mathbf{V}, \qquad (5.2)$$

$$T = \frac{1}{3nk_b} \int_{R^3} \mathcal{F} v_j' v_j' d^3\mathbf{V}, \qquad (5.5)$$

$$\langle \psi(\mathbf{M}) \rangle = \frac{1}{\rho} \int_{R^3} \phi(\mathbf{V}) \mathcal{F} d^3\mathbf{V}, \qquad (5.3)$$

$$\pi_{ij} = \int_{R^3} \mathcal{F} v'_{\langle i} v'_{j \rangle} d^3\mathbf{V} \text{ and} \qquad (5.6)$$

$$U_i = \frac{1}{\rho} \int_{R^3} \mathcal{F} V_i d^3\mathbf{V}, \qquad (5.4)$$

$$q_i = \frac{1}{2} \int_{R^3} \mathcal{F} v_i' v_j' v_j' d^3\mathbf{V}. \qquad (5.7)$$

- **If we know evolution of $\mathcal{F}$, we know future macroscopic states of the system**.
- Generic form of the evolution of distribution function of each particle in non-equilibrium gas

$$\frac{\partial \mathcal{F}}{\partial t} + \frac{\partial (\mathcal{F} V_i)}{\partial x_i} + \frac{\partial (\mathcal{F} G_i)}{\partial V_i} = S_{coll}(\mathcal{F}) \ . \tag{5.8}$$

- $S_{coll}(\mathcal{F})$ collision operator accounting for the binary collisions among molecules and **G** the external force.
- $S_{coll}(\mathcal{F})$ is the Boltzmann operator for dilute gas and the Enskog operator for dense gases.

Enskog operator[6]

- With simple modification to the Boltzmann operator

$$S^{Enskog} = \int_{\mathbb{R}^3}\int_0^{2\pi}\int_0^{+\infty}\Big[Y(\mathbf{x}+\frac{1}{2}\sigma\hat{\mathbf{k}})\mathcal{F}(\mathbf{V}^*,\mathbf{x})\mathcal{F}(\mathbf{V}_1^*,\mathbf{x}+\sigma\hat{\mathbf{k}}) - Y(\mathbf{x}-\frac{1}{2}\sigma\hat{\mathbf{k}})\mathcal{F}(\mathbf{V},\mathbf{x})\mathcal{F}(\mathbf{V}_1,\mathbf{x}-\sigma\hat{\mathbf{k}})\Big] g\hat{b}d\hat{b}d\hat{\epsilon}d^3\mathbf{V}_1, \quad (5.9)$$

where

$$Y = 1 + 0.625nb + 0.2869(nb)^2 + 0.115(nb)^3 \text{ and} \quad (5.10)$$

$$b = \frac{2}{3}\pi\sigma^3. \quad (5.11)$$

- Assumptions:
  1- Volume occupied by the molecules becomes comparable with the whole volume of the gas which leads to the factor Y in collision rate.
  2- VDF of colliding pair must be in vicinity of each other, exactly σ for HS, for collisions to happen.

[6] see Chapman and Cowling (1953) [7] and Hirschfelder et al. (1963) [8].

From statistical mechanics, the virial expansion of pressure can be obtained by

$$Z := \frac{p}{nkT} = 1 + B_2 n + B_3 n^2 + B_4 n^2 ..., \tag{5.12}$$

$$B_N = \frac{1-N}{N!} \lim_{V \to 0} V^{-1} \int ... \int d\mathbf{r}_1 ... d\mathbf{r}_N V_N, \tag{5.13}$$

$$V_N = \sum \prod_{i<j}^{N} f_{ij} \tag{5.14}$$

$$\text{and} \quad f_{ij} = exp(-\phi_{ij}/kT) - 1, \tag{5.15}$$

where ϕ_{ij} is molecular potential between particles i and j.

The factor Y (which comes form virial expansion)

$$Y := \frac{Z-1}{nb} \tag{5.16}$$

for hard-sphere can be calculated exactly as done by Ree-Hoover [13]

$$Y = 1 + 0.625nb + 0.2869(nb)^2 + 0.115(nb)^3 + ... \tag{5.17}$$

or approximated by a closed expression as suggested by Carnahan-Starling [14]

$$Y^{CS} = \frac{1 - nb/8}{(1 - nb/4)^3}. \tag{5.18}$$

- Now we know what we want to solve.
- Boltzmann and Enskog equations are difficult to solve directly due to high dimensionalily of $\mathcal{F}(\mathbf{V}, \mathbf{x}, t)$.
- Monte-Carlo methods are suggested in literature as an efficient yet accurate alternative compared to direct solution method and moment approach.

Outline

Direct Simulation Monte Carlo (DSMC[8])

- Positions and velocities are updated in two steps: **streaming** and **collision**.
- Collision involves picking Λ_{coll} couple of particles as candidates

$$\Lambda_{max} = F_N N_C^2 \pi \sigma^2 M_{r,max} \Delta t / V_c. \tag{5.19}$$

- Selected pair collide if

$$M_r / M_{r,max} > r, \tag{5.20}$$

  then velocities change such that

$$\mathbf{M}_r^{post} = M_r^{post} (cos\theta, sin\theta cos\phi, sin\theta sin\phi)^T, \tag{5.21}$$

$$\phi = 2\pi\alpha_1 \quad \text{and} \tag{5.22}$$

$$cos\theta = 1 - 2\alpha_2, \tag{5.23}$$

  with α_1 and α_2 being uniform random numbers between zero and one.
- DSMC is proven to be consistent with the Boltzmann equation[7].

[7] Wanger (1992) [15].

[8] Bird (1963) [16].

Consistent Boltzmann Algorithm (CBA[9])

- **With two modifications in DSMC, one can model dense gas!**
- Collision rate needs to be increased by Y,

$$\Lambda^{CBA} = {\color{red}Y} F_N N_C^2 \pi \sigma^2 M_{r,max} \Delta t / V_c. \tag{5.24}$$

- Additional advection due to diameter effect in streaming

$$\mathbf{d} = \frac{\mathbf{M}_r^* - \mathbf{M}_r}{||\mathbf{M}_r^* - \mathbf{M}_r||_2}\sigma, \tag{5.25}$$

$$\mathbf{X}_1 = \mathbf{M}_1 \Delta t {\color{red}+\mathbf{d}} \quad \text{and} \tag{5.26}$$

$$\mathbf{X}_2 = \mathbf{M}_2 \Delta t {\color{red}-\mathbf{d}}. \tag{5.27}$$

- CBA loses consistency as density increases ($n\sigma^3 > 0.4$).

Complexity of Monte Carlo methods

Complexity scales with $\mathcal{O}(n^2)$, where n is number density.

[9] see Alexander et al. (1995) [17].

Enskog Simulation Monte-Carlo (ESMC[10])

- ESMC was proposed as an accurate solution to Enskog equation.
- Collision rate is increased by a Y factor, i.e. $\Lambda^{Ensk} = Y\Lambda^{Boltz}$.
- Modification in selection of collision pair:
  - Pick a particle ($\mathbf{x}_i$) at random.
  - Pick a random direction $\hat{\boldsymbol{\sigma}}$. Then, find the second particle ($\mathbf{x}_j$) in the cell that $\mathbf{x}_i + \sigma\hat{\boldsymbol{\sigma}}$ exists.
  - Find Y at the mid point and update Λ^{Ensk} if necessary. Calculate $\Gamma = 4\pi\sigma^2(\mathbf{M}_\mathbf{r}.\hat{\boldsymbol{\sigma}})Y_{mid}\Delta t$.
  - If $\Gamma/\Gamma_{max} > r$, accept the collision and set $\mathbf{M}_i^* = \mathbf{M}_i - (\mathbf{M}_\mathbf{r}.\hat{\boldsymbol{\sigma}})\hat{\boldsymbol{\sigma}}$.

Complexity of Monte Carlo methods

Complexity scales with $\mathcal{O}(n^2)$, where n is number density.

[10] see Montanero and Santos (1996) [9].

- As mentioned, computational cost of DSMC's based methods increases as gas gets denser.
- It is because collision rate increases with density.
- However, FP model does not suffer from this problem.
- Therefore, it is worth expanding FP model for dense gases.

Outline

Review: Fokker-Planck model for ideal gas

- For an Itô process

$$d\mathbf{p} = \widetilde{\mathbf{A}}dt + \boldsymbol{\lambda}d\mathbf{W}, \tag{5.28}$$

where $\mathbf{W}$ is a Wiener process and

$$\mathbf{p} = \begin{pmatrix} M_1 \\ M_2 \\ M_3 \\ X_1 \\ X_2 \\ X_3 \end{pmatrix}, \boldsymbol{\lambda} = \begin{pmatrix} D_{11} & D_{12} & D_{13} & 0 & 0 & 0 \\ D_{21} & D_{22} & D_{23} & 0 & 0 & 0 \\ D_{31} & D_{32} & D_{33} & 0 & 0 & 0 \\ 0 & 0 & 0 & 0 & 0 & 0 \\ 0 & 0 & 0 & 0 & 0 & 0 \\ 0 & 0 & 0 & 0 & 0 & 0 \end{pmatrix} \text{ and } \quad \widetilde{\mathbf{A}} = \begin{pmatrix} A_1 \\ A_2 \\ A_3 \\ M_1 \\ M_2 \\ M_3 \end{pmatrix}, \tag{5.29}$$

Itô calculus provides us the equivalent Fokker-Planck equation[11]

$$\frac{\partial \mathcal{F}}{\partial t} + \frac{\partial(\mathcal{F}V_i)}{\partial x_i} = -\frac{\partial(\mathcal{F}A_i)}{\partial V_i} + \frac{1}{2}\frac{\partial^2}{\partial V_i \partial V_j}(D_{ik}D_{kj}\mathcal{F}). \tag{5.30}$$

Drift and diffusion

A_i and D_{ij} are called drift and diffusion coefficients, respectively. They are set to give stochastics of S_{coll}.

[11] see Gardiner (1996) [11].

Review: linear FP for ideal gas

- Jenny *et al.* (2010) [18] considered a Langevin model

$$A_i = -\frac{1}{\tau} v_i' \quad \text{and} \quad D_{ij} = \sqrt{\frac{2kT}{\tau m}} \delta_{ij}, \tag{5.31}$$

with $\tau = 2\mu^{\text{kin}}/p$.

- Linear model is consistent with the Boltzmann equation up to second velocity moment, i.e. $\psi \in \{1, V_i, V_i V_j\}$.
- It was shown that the linear FP produces inconsistent relaxation rates for shear stress and heat fluxes, consequently inconsistent Prandtl number in hydrodynamic limit.

Review: cubic FP model for ideal gas

- In order to provide consistent relaxation rates, Cubic FP was designed by Gorji *et al.* (2011) [12]

$$
\begin{aligned}
A_i &= c_{ij} v'_j + \gamma_i \left(v'_j v'_j - \frac{3kT}{m} \right) + \Lambda \left(v'_i v'_j v'_j - \frac{2q_i}{\rho} \right) \quad , &(5.32)\\
D_{ij} &= \sqrt{\frac{2kT}{\tau m}} \delta_{ij} \quad \text{and} &(5.33)\\
\tau &= 2\mu^{\text{kin}}/p \ , &(5.34)
\end{aligned}
$$

where coefficients of higher order terms $\mathbf{c}$ and γ are set satisfying homogeneous relaxation rates[12],

$$
\begin{aligned}
\frac{\partial \pi_{ij}}{\partial t} &= -\frac{p}{\mu} \pi_{ij} \ \text{and} &(5.35)\\
\frac{\partial q_i}{\partial t} &= -\frac{2}{3} \frac{p}{\mu} q_i . &(5.36)
\end{aligned}
$$

[12] see Truesdell and Muncaster (1980) [19].

Conditions on any S_{coll} describing monatomic dilute gas:

- S_{coll} must conserve mass, momentum an energy i.e. for any $\Psi_{cons} \in \{1, V_i, V_j V_j\}$

$$\int_{\mathbb{R}^3} \Psi_{cons} S_{coll}(\mathcal{F}) d^3\mathbf{V} = 0 \quad \text{for any} \quad \mathcal{F}. \tag{5.37}$$

- Considering a homogeneous setting, the equilibrium is a Maxwellian distribution

$$S(\mathcal{F}) = 0 \rightarrow \mathcal{F} = \mathcal{F}_M. \tag{5.38}$$

- In order to obtain identical transport properties

$$\int_{\mathbb{R}^3} \Psi S^{model}(\mathcal{F}) d^3\mathbf{V} = \int_{\mathbb{R}^3} \Psi S_{coll}(\mathcal{F}) d^3\mathbf{V}, \tag{5.39}$$

where $\Psi = \{V_i V_j, V_i V_j V_k, ..., V_{i_1} ... V_{i_M}\}$.

- Relaxation rates of the shear stress and the heat fluxes must be[13]

$$\frac{\partial \pi_{ij}}{\partial t} = -\frac{P}{\mu}\pi_{ij} \quad \text{and} \tag{5.40}$$

$$\frac{\partial q_i}{\partial t} = -\frac{2}{3}\frac{P}{\mu} q_i \ . \tag{5.41}$$

A Fokker-Planck model for dense gases

Outline

Homogeneous relaxation rates of Enskog equation

- Let us simplify Enskog operator using the decomposition

$$S^{\text{Enskog}} = Y(\mathbf{x})S^{\text{Boltz}} + S_\phi \tag{6.1}$$

where S_ϕ includes all derivative of $\mathcal{F}$ and Y in $\mathbf{x}$.

- Relaxation rates of shear stress and heat fluxes then become

$$\frac{\partial \pi_{ij}}{\partial t} = -Y\frac{p}{\mu^{\text{kin}}}\pi_{ij} \tag{6.2}$$

$$\text{and} \quad \frac{\partial q_i}{\partial t} = -Y\frac{2}{3}\frac{p}{\mu^{\text{kin}}}q_i \ , \tag{6.3}$$

- Drift and diffusion coefficients of cubic model of **A** must satisfy this relaxation rates for dense gases.
- Spatial dependence of Enskog operator needs to be modeled.

Conservation equations of Enskog equation

Taking velocity moments $\psi \in \{1, V_j, V_j V_j/2\}$ of S^{Ensk}

$$J = \int_{\mathbb{R}^3} \psi S^{\text{Ensk}} d^3\mathbf{V}. \tag{6.4}$$

Deploying Taylor expansion near $\mathbf{x}$ for $\mathcal{F}$ and Y

$$J = J_0 + J_1 + J_2 + ... \tag{6.5}$$

where for $Y = Y(\mathbf{x})$, $\mathcal{F} = \mathcal{F}(\mathbf{V}^*, \mathbf{x})$ and $\mathcal{F}_1 = \mathcal{F}(\mathbf{V}_1^*, \mathbf{x})$

$$J_0 = 0, \tag{6.6}$$

$$J_1 = -\frac{\partial}{\partial x_i}\Big[\frac{\sigma}{2}\int\int\int\int(\psi^* - \psi) Y \mathcal{F}\mathcal{F}_1 k_i g \hat{b} d\hat{b} d\hat{\epsilon} d^3\mathbf{V}_1 d^3\mathbf{V}\Big], \tag{6.7}$$

$$J_2 = -\frac{\partial}{\partial x_i}\Big[\frac{\sigma^2}{4}\int\int\int\int(\psi^* - \psi) Y \mathcal{F}\mathcal{F}_1 \frac{\partial}{\partial x_j}(ln\frac{\mathcal{F}}{\mathcal{F}_1}) k_i k_j g \hat{b} d\hat{b} d\hat{\epsilon} d^3\mathbf{V}_1 d^3\mathbf{V}\Big]. \tag{6.8}$$

Conservation equations of Enskog equation

- Taking velocity moment $\psi \in \{1, V_j, V_j V_j/2\}$ of expanded Enskog equation leads to

$$\int_{\mathbb{R}^3} \psi\left(\frac{\partial \mathcal{F}}{\partial t} + V_i \frac{\partial \mathcal{F}}{\partial x_i}\right) d^3\mathbf{V} \quad = -\frac{\partial \Psi_i^\phi}{\partial x_i}. \tag{6.9}$$

By keeping only first derivatives in Taylor expansion, one can show

$$\Psi_i^\phi = \frac{Y\sigma}{2} \int\int\int\int (\psi^* - \psi)\mathcal{F}\mathcal{F}_1 g\hat{b}d\hat{b}d\hat{\epsilon}d^3\mathbf{V}_1 d^3\mathbf{V} + \frac{Y\sigma^2}{4} \int\int\int\int (\psi^* - \psi)k_i\mathcal{F}\mathcal{F}_1 \frac{\partial}{\partial x_i} ln\left(\frac{\mathcal{F}}{\mathcal{F}_1}\right) g\hat{b}d\hat{b}d\hat{\epsilon}d^3\mathbf{V}_1 d^3\mathbf{V}. \tag{6.10}$$

- Unlike Boltzmann, moments of Enskog operator does not vanish! This contribution is called **Collisional Transfer**.

- Ψ_i^{ϕ} is approximated by Chapmann and Cowling[14]
  - Ignoring Higher order terms.
  - $\partial_{\mathbf{x}} ln(\mathcal{F}/\mathcal{F}_1) \approx \partial_{\mathbf{x}} ln(\mathcal{F}^0/\mathcal{F}_1^0)$, where $\mathcal{F}^0$ is the Maxwelllian VDF.

Mass Conservation:

$$\frac{\partial \rho}{\partial t} + \frac{\partial}{\partial x_j}(\rho U_j) = 0. \quad (6.11)$$

Momentum Conservation:

$$\frac{\partial}{\partial t}(\rho U_i) + \frac{\partial}{\partial x_j}\left(\rho U_i U_j + \pi_{ij}^{tot} + p^{tot}\delta_{ij}\right) = 0. \quad (6.12)$$

Energy Conservation:

$$\frac{\partial E}{\partial t} + \frac{\partial}{\partial x_i}\left(EU_i + q_i^{tot} + p^{tot}\delta_{ik}U_k + \pi_{ik}^{tot}U_k\right) = 0, \quad (6.13)$$

where $E = \rho c_v T + \frac{1}{2}\rho U_k U_k$ and $c_v = 3k/(2m)$.

[14] see Chapman and Cowling (1953) [7]

- Therefore, total pressure tensor and heat fluxes can be derived

$$p^{\text{tot}} = nkT(1+nbY) - w\frac{\partial U_k}{\partial x_k}, \tag{6.14}$$

$$\pi_{ij}^{\text{tot}} = (1+2nbY/5)\pi_{ij} - (5w/6)\frac{\partial U_{\langle i}}{\partial x_{j\rangle}} \tag{6.15}$$

and

$$q_i^{\text{tot}} = (1+3nbY/5)q_i - c_v w\frac{\partial T}{\partial x_i}. \tag{6.16}$$

with $w = (nb)^2 Y\sqrt{mkT}/(\pi^{3/2}\sigma^2)$ being bulk effect.

- We use these expressions to correct pressure tensor and heat fluxes in FP of dense gases.

Outline

FP of dense gases - Modification in Velocity Update

- To guarantee relaxation rates of Enskog operator

$$\frac{\partial \pi_{ij}}{\partial t} = -Y \frac{p}{\mu} \pi_{ij} \quad \text{and} \tag{6.17}$$

$$\frac{\partial q_i}{\partial t} = -Y \frac{2}{3} \frac{p}{\mu} q_i \ , \tag{6.18}$$

Cubic drift **A** for dense gas should now satisfy

$$\rho \langle A_i M'_j + A_j M'_i + D^2 \delta_{ij} \rangle = -Y \frac{P}{\mu} \pi_{ij} \ \text{and} \tag{6.19}$$

$$\rho \langle A_i M'_j M'_j + 2A_j M'_j M'_i \rangle = -Y \frac{2}{3} \frac{p}{\mu} q_i. \tag{6.20}$$

Outline

FP with collisional transfer

- Collisional transfer promotes idea of extra streaming

$$\frac{\partial \mathcal{F}}{\partial t} + \frac{\partial(\mathcal{F}V_i)}{\partial x_i} = -\frac{\partial(\mathcal{F}A_i)}{\partial V_i} + \frac{1}{2}\frac{\partial^2(D^2\mathcal{F})}{\partial V_j \partial V_j} - \frac{\partial(\mathcal{F}\hat{A}_i)}{\partial x_i} \ . \qquad (6.21)$$

- What is $\hat{\mathbf{A}}$?
  Answer: $\hat{\mathbf{A}}$ is a spatial drift which should be set such that moments of FP matches moments of Enskog, i.e. provides correction to total pressure tensor and heat fluxes.
- In this study, we proposed a linear and a cubic model for $\hat{\mathbf{A}}$.

Linear DFP

- Consider the linear ansatz $\hat{\mathbf{A}}$

$$\hat{A}_i = \alpha v_i' \ . \tag{6.22}$$

- *Conservation of mass:*

$$\frac{\partial \rho}{\partial t} + \frac{\partial (\rho U_i)}{\partial x_i} = 0 \ . \tag{6.23}$$

- *Conservation of momentum:*

$$\frac{\partial (\rho U_i)}{\partial t} + \frac{\partial}{\partial x_j}(\rho U_i U_j + \pi_{ij} + p\delta_{ij}) + \frac{\partial}{\partial x_j} \int_{\mathbb{R}^3} \hat{A}_j V_i \mathcal{F} d^3\mathbf{V} = 0 \ . \tag{6.24}$$

- Total pressure p^{tot} of Enskog equation can be achieved by setting

$$\alpha = nbY - \frac{w}{nkT}\frac{\partial U_i}{\partial x_i}. \tag{6.25}$$

Cubic DFP

- Consider a cubic model for $\hat{\mathbf{A}}$

$$\begin{aligned}\hat{A}_i &= \hat{c}_{ij} v'_j + \hat{\gamma}_i \left(v'_j v'_j - \frac{3kT}{m} \right) \\ &+ \hat{\Lambda} \left(v'_i v'_j v'_j - \frac{2q_i}{\rho} \right) \end{aligned} \tag{6.26}$$

  where quadratic term is used to set total heat flux and cubic term with $\hat{\Lambda} = -\epsilon nbY/(kT/m)$ is set to avoid instabilities of SDEs[15].
- Conservation of mass

$$\frac{\partial \rho}{\partial t} + \frac{\partial (\rho U_i)}{\partial x_i} = 0 \ . \tag{6.27}$$

[15] see Risken (1989) [20].

Cubic DFP: conservation of momentum

- First velocity moment of DFP leads to

$$\frac{\partial}{\partial t}(\rho U_i) + \frac{\partial}{\partial x_j}(\rho U_i U_j) + \frac{\partial}{\partial x_j}(\pi_{ij} + p\delta_{ij}) + \frac{\partial}{\partial x_j}\left(\hat{c}_{jk}\pi_{ik} + \hat{c}_{ji}p + 2\hat{\gamma}_j q_i + \rho\hat{\Lambda}u_{ij}^{(2)}\right) = 0 \,. \quad (6.28)$$

Coefficients of spatial drift $\hat{\mathbf{c}}$ and $\hat{\gamma}$ are set to obtain total pressure and stress tensor of Enskog equation

$$\hat{c}_{jk}\pi_{ik} + \hat{c}_{ji}p + 2\hat{\gamma}_j q_i = -\rho\hat{\Lambda}u_{ij}^{(2)} + nbY(p\delta_{ij} + 2/5\pi_{ij}) - w\left(\frac{\partial U_k}{\partial x_k}\delta_{ij} + \frac{5}{6}\frac{\partial U_{\langle i}}{\partial x_{j\rangle}}\right) . (6.29)$$

Cubic DFP: conservation of energy

- Second velocity moment of DFP provides

$$\frac{\partial E}{\partial t} + \frac{\partial}{\partial x_i}\left(EU_i + q_i + p\delta_{ik}U_k + \pi_{ik}U_k\right) + \frac{1}{2}\frac{\partial}{\partial x_i}\int_{\mathbb{R}^3} \hat{A}_i V_k V_k \mathcal{F} d^3\mathbf{V} = 0. \quad (6.30)$$

Substituting $\hat{\mathbf{A}}$, one can set heat fluxes of DFP to match $\mathbf{q}^{\text{tot}}$

$$\hat{c}_{ij}q_j + \frac{1}{2}\rho\hat{\gamma}_i\left(u^{(4)} - (u^{(2)})^2\right) = \frac{3}{5}nbYq_i - wc_v\frac{\partial T}{\partial x_i} - \frac{1}{2}\rho\hat{\Lambda}\left(u_i^{(4)} - u_i^{(2)}u^{(2)}\right). \quad (6.31)$$

Cubic FP: coefficients

- From momentum conservation

$$\begin{aligned} \hat{c}_{jk}\pi_{ik} &+ \hat{c}_{ji}p + 2\hat{\gamma}_j q_i = -\rho\hat{\Lambda}u_{ij}^{(2)} \\ &+ nbY(p\delta_{ij} + 2/5\pi_{ij}) - w\left(\frac{\partial U_k}{\partial x_k}\delta_{ij} + \frac{5}{6}\frac{\partial U_{\langle i}}{\partial x_{j\rangle}}\right). (6.32) \end{aligned}$$

- From energy conservation:

$$\begin{aligned} \hat{c}_{ij}q_j &+ \frac{1}{2}\rho\hat{\gamma}_i\left(u^{(4)} - (u^{(2)})^2\right) \\ &= \frac{3}{5}nbYq_i - wc_v\frac{\partial T}{\partial x_i} - \frac{1}{2}\rho\hat{\Lambda}\left(u_i^{(4)} - u_i^{(2)}u^{(2)}\right). \quad (6.33) \end{aligned}$$

Notation

- Following notation was used in the formulations.

$$u^{(k)}_{i_1 \dots i_n} = \frac{1}{\rho} \int_{\mathbb{R}^3} |\mathbf{v'}|^k v'_{i_1} v'_{i_2} \dots v'_{i_n} \mathcal{F} d^3\mathbf{V}. \qquad (6.34)$$

Outline

Reduction to SDEs

Using Itô calculus, equivalent Itô process of DFP is

$$d\mathbf{p} = \widetilde{\mathbf{A}}dt + \boldsymbol{\lambda} d\mathbf{W}, \tag{6.35}$$

where **W** is a Wiener process and

$$\mathbf{p} = \begin{pmatrix} M_1 \\ M_2 \\ M_3 \\ X_1 \\ X_2 \\ X_3 \end{pmatrix}, \quad \boldsymbol{\lambda} = \begin{pmatrix} D & 0 & 0 & 0 & 0 & 0 \\ 0 & D & 0 & 0 & 0 & 0 \\ 0 & 0 & D & 0 & 0 & 0 \\ 0 & 0 & 0 & 0 & 0 & 0 \\ 0 & 0 & 0 & 0 & 0 & 0 \\ 0 & 0 & 0 & 0 & 0 & 0 \end{pmatrix} \text{ and } \quad \widetilde{\mathbf{A}} = \begin{pmatrix} A_1 \\ A_2 \\ A_3 \\ M_1 + \hat{A}_1 \\ M_2 + \hat{A}_2 \\ M_3 + \hat{A}_3 \end{pmatrix}. \tag{6.36}$$

Outline

Numerical Scheme

Explicit scheme for velocity update[16], and Euler method for position update are employed as in

$$M_i^{n+1} = U_i^n + \alpha_{cell}\Big(M_i'^n e^{-\Delta t Y/\tau} + c_{ik} M_k'^n + \gamma_i (M_k'^n M_k'^n - 3kT/m) + \Lambda(M_i'^n M_j'^n M_j'^n - \langle M_i'^n M_j'^n M_j'^n \rangle) + \sqrt{\frac{2kTY}{\tau m}}\xi_i\Big) \text{ and} \quad (6.37)$$

$$X_i^{n+1} = X_i^n + M_i^n \Delta t + \Big(\hat{c}_{ij} M_j'^n + \hat{\gamma}(M_j'^n M_j'^n - 3kT/m) + \hat{\Lambda}(M_i'^n M_j'^n M_j'^n - \langle M_i'^n M_j'^n M_j'^n \rangle)\Big)\Delta t. \quad (6.38)$$

α_{cell} makes sure that kinetic energy in each cell is conserved,

$$\alpha_{cell} = \frac{\langle M_k'^n M_k'^n \rangle}{\langle M_k'^{n+1} M_k'^{n+1} \rangle} \ . \quad (6.39)$$

[16] similar to Gorji and Jenny (2014) [21].

Outline

Setup

- Consider a gas contained in a box with iso-thermal walls that can be moved. Velocity of particles hitting the walls in x_2 are set to the velocity of equilibrium distribution on the face[17], i.e.

$$M_1 = \sqrt{\frac{k_b T_w}{m}}\mathcal{N}(0,1) \pm U_w, \tag{7.1}$$

$$M_2 = \pm\sqrt{\frac{2k_b T_w}{m}}\sqrt{-ln\Big(\mathcal{R}(0,1)\Big)} \text{ and} \tag{7.2}$$

$$M_3 = \sqrt{\frac{k_b T_w}{m}}\mathcal{N}(0,1). \tag{7.3}$$

[17] see Bird (1994) [22].

Setup

- In all simulations, Argon is used with[18]

μ $[kg.m^{-1}.s^{-1}]$	ω $[-]$	σ $[m]$	m $[kg]$	κ $[W.m^{-1}.K^{-1}]$
2.117×10^{-5}	0.5	3.628×10^{-10}	6.633×10^{-26}	0.01625

- Time step is picked based on CFL condition[19]

$$\Delta t = 0.05 \frac{min(\lambda, L/n_c)}{max(U_w, U_{th})} \tag{7.4}$$

for DSMC's based methods and

$$\Delta t = 0.05 \frac{L/n_c}{max(U_w, U_{th})} \tag{7.5}$$

for FP based methods.

[18] see Bird (1963) [22].

[19] see Gorji and Jenny (2015) [23].

Outline

Equilibrium Pressure

- Iso-thermal constant walls with $T_w = 273\ K$.
- Pressure can be calculated based on its fundamental definition

$$p = \frac{1}{At^f}\Big(\sum_{t=0}^{t^f}\sum_{j=1}^{N_c}\Delta(mM_j)\Big). \tag{7.6}$$

Dashed and solid lines are $p = nkT$ and $p = nkT(1 + nbY)$.

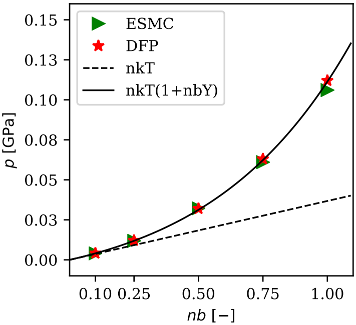

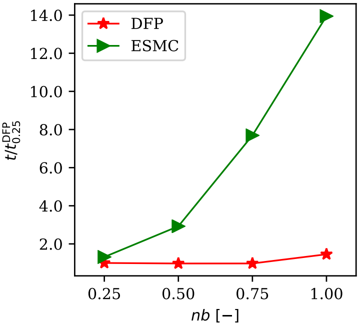

Outline

Couette flow

- Iso-thermal walls at $T = 273\ K$ are moved $U_w = (\pm 150, 0, 0)^T\ [m/s]$.
- Here, $Kn = 0.01$ and $nb = 0.5$.
- Convergence studies on the spatial refinement lead us to 100 computational cells in x_2. 1000 particles per cell are employed.
- Solid lines $\mu_0^{\mathrm{tot}} = \mu_0^{\mathrm{kin}}(1 + 2n_0 b Y_0/5)^2/Y_0 + 3w_0/5$ and dashed line indicates μ^{kin}.

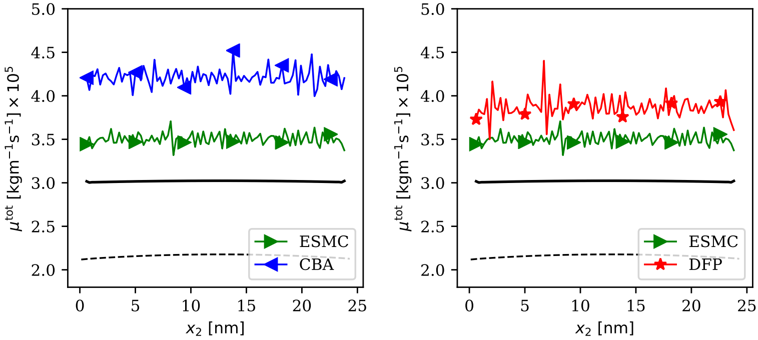

Outline

Fourier flow

- Iso-thermal constant walls with $T_{w1} = 300\ K$ and $T_{w2} = 500\ K$.
- Here, $Kn = 0.01$ and $nb = 0.5$.
- Convergence studies gives us 100 cells in x_2.
- Solid lines $\kappa_0^{\text{tot}} = \kappa_0^{\text{kin}}(1 + 3n_0bY_0/5)^2/Y_0 + w_0c_v$ and dashed line indicates κ_0^{kin}.

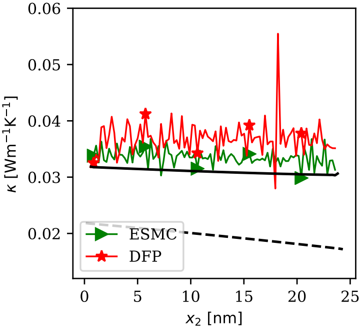

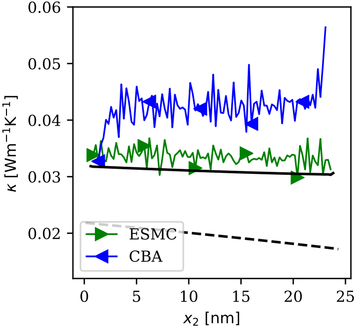

Conclusion

- We proposed a Fokker-Planck model suitable for dense gas.
- Dense gas effects were captured by introducing a spatial drift term.
- Several examples showed the accuracy of model in capturing total pressure, shear stress and heat fluxes.

Outlooks

- Hard Sphere (what we assumed here according to Enskog operator) is not so accurate representation of force field in very dense gases or liquids. A collision operator based on more realistic molecular potentials, such as Lennard-Jones potential, is needed.
- More accurate time integration scheme can let us increase time step.
- Idea of extra streaming might provide a framework for modeling incompressible constraint with Fokker-Planck.

Thanks for your attention.

Any questions?

Measurement of gradient

$$\langle \mathbf{Q} \rangle = \frac{\sum_{j=1}^{N_c} \mathbf{Q}_j}{N_c} \ . \tag{8.1}$$

$$\frac{\partial Q_i}{\partial x_j} \approx \frac{\int \frac{\partial Q_i}{\partial x_j} dV}{\int dV} = \frac{\oint Q_i n_j dA}{\Delta V} \ . \tag{8.2}$$

$$\langle Q_i \rangle_f = \frac{\sum_{j=1}^{N_c} Q_i^j \delta t^j}{\sum_{j=1}^{N_c} \delta t^j} = \frac{\sum_{j=1}^{N_c} Q_i^j \frac{\delta x_i}{M_i^j}}{\sum_{j=1}^{N_c} \frac{\delta x_i}{M_i^j}} \ . \tag{8.3}$$